Magnetic-ion triplet clusters and non-nearest-neighbor exchange effect in (Cd,Mn)Te

Xiaomei Wang,* D. Heiman, S. Foner,* and P. Becla

Francis Bitter National Magnet Laboratory, Massachusetts Institute of Technology, Cambridge, Massachusetts 02139

(Received 23 June 1989)

Internal quantum structures of Mn^{2+} spin clusters in $Cd_{1-x}Mn_xTe$ are studied by Faraday-rotation measurements up to 60 T at $T \sim 4$ K. For $x = 0.1$ we observe the contribution of Mn^{2+} triplet clusters, as well as the saturation of Mn^{2+} pairs. Overall good agreement between the experiments and a nearest-neighbor cluster model is obtained. By quantitative analysis of the data for pairs, we find a linear relation between bias field (average exchange field due to more-distant interactions) and total magnetization, independent of x (for $x \leq 0.1$). This relation allows us to determine the strength of next-nearest-neighbor interactions, $J_2/k_B = -1.1$ K.

Dilute magnetic semiconductors (DMS), such as $Cd_{1-x}Mn_xTe$, are excellent hosts for the study of disordered magnetic systems. These materials clearly show the internal quantum structure of spin clusters. Here a cluster is defined as a group of magnetic ions on a face-centered-cubic cation sublattice, connected by nearest-neighbor (NN) "bonds." The NN spin-exchange interactions are usually much larger than more-distance interactions. A number of experiments[1-8] have been devoted to the investigation of the NN exchange constant J_1 of magnetic ion pairs, including recent spin-flip Raman scattering,[7] and pulsed-field magnetization measurements[8] by us. As the magnetic field B increases, the spin alignment (magnetization) of antiferromagnetically coupled pairs exhibits a series of steplike increases. For Mn^{2+} ions with $S = \frac{5}{2}$, these steps occur at transition fields B_n as the ground state (with total spin S_T and z-component m) changes from $|S_T, m\rangle = |0, 0\rangle$, through $|1, -1\rangle, \ldots,$ $|5, -5\rangle$. Analysis of the magnitudes of these transition fields in dilute samples ($x < 0.05$) gives accurate values of J_1. In (Cd,Mn)Te, $J_1/k_B = -6.1$ K, so that the first pair step occurs at ~ 10 T and the fifth step[8] occurs at $B \sim 50$ T.

Here we provide quantitative evidence of magnetic ion triplets, and of the saturation of magnetic ion pairs. Magnetization measurements using a Faraday-rotation technique on (Cd,Mn)Te up to 60 T at liquid-helium temperature are reported. The measured magnetization $M(B)$ versus field B is composed of three different linear regimes. The changes of slope correspond to the onset of triplets and the saturation of pairs. Quantitative agreement with the experimental results is found for the NN cluster model. Further-neighbor interactions are included by introducing an average biasing exchange field Δ. We find a linear relationship between Δ and M for ion pairs, independent of manganese concentration x for $x \leq 0.1$. From this relation, we deduce the next-nearest-neighbor (NNN) exchange constant $J_2/k_B = -1.1$ K.

There are two types of magnetic ion triplet clusters— open triplets and closed triplets as illustrated in Table I. In the dilute limit the probability of triplets is low in comparison with that of singlets or pairs. To increase the
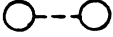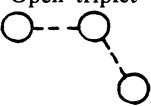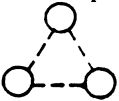
probability of triplets without excessively broadening the structure in $M(B)$, we chose samples with manganese concentration $x = 0.1$. At this concentration the probabilities that a Mn^{2+} ion belongs to a singlet, pair, and triplets are 0.28, 0.18, 0.09 (open triplet), and 0.02 (closed triplet), respectively. The remaining ions are in larger clusters having total probability of 0.43. To distinguish triplets from singlets and pairs, we recognize that the series of steps in $M(B)$ for open triplets starts at much higher field ~ 30 T (compared with ~ 10 T for pairs), due to their larger ground-state total spin at zero field, $S_T = \frac{5}{2}$ (compared with $S_T = 0$ for pairs). At 4 K these equal-step ladders are broadened into linear trends and the structure of $M(B)$ is simplified. Thus the additional contribution of a linear trend from triplets results in an upward turn or kink in $M(B)$ at ~ 30 T. Below we outline the theoretical background and discuss our experimental results.

In the nearest-neighbor interaction model,[9] the magnetic structure is composed of a collection of isolated clusters. For low magnetic ion concentration ($x \leq 0.1$), small clusters such as singlets, pairs, and triplets dominate the magnetic ion population; their associated eigenenergies can be calculated from the Hamiltonian listed in Table I. A random spatial distribution of magnetic ions on the fcc cation sublattice is assumed. With knowledge of these microscopic properties, we obtain M as a function of B and temperature T through general thermal ensemble theory:

$$M_i = \left[\frac{A}{W}x\right]\left[\frac{P_i}{n_i}\right]g\mu_B \frac{\sum\limits_{\{l\}_i} -m e^{-\beta E_i(\{l\})}}{\sum\limits_{\{l\}_i} e^{-\beta E_i(\{l\})}}, \quad (1)$$

where A is Avogadro's number, W is the formula molecular weight in grams per mole, $g = 2.0$, $S = \frac{5}{2}$ for Mn^{2+}; $E_i(\{l\})$ (see Table I) are eigenenergies and M_i the magnetization of clusters of type i ($i = s, p$, ot, and ct for singlets, pairs, open, and closed triplets, respectively), P_i is the probability of finding a magnetic ion in the type-i cluster evaluated from Ref. 10; and n_i is the number of ions in that type of cluster. The summation is over all

TABLE I. Hamiltonians, eigenenergies (Ref. 9), and ground-state transition fields (Ref. 1) B_n for small clusters with ion spin $S = \frac{5}{2}$ in the NN model.

Cluster	Hamiltonian and eigenenergy	Transition fields
Singlet $\bigcirc$	$H = g\mu_B S^z B$ $E(S_T, m) = g\mu_B m B$ $S_T = \frac{5}{2}, \quad |m| \leq S_T$	
Pair $\bigcirc\text{--}\bigcirc$	$H = -2J_1(\mathbf{S}_1 \cdot \mathbf{S}_2) + g\mu_B(S_1^z + S_2^z)B$ $E(S_T, m) = -J_1[S_T(S_T+1) - \frac{35}{2}] + g\mu_B m B$ $\mathbf{S}_T = \mathbf{S}_1 + \mathbf{S}_2$ $0 < S_T < 5, \quad |m| \leq S_T$	$B_n = 2n|J_1|/g\mu_B$ $n = 1, \ldots, 5$
Open triplet $\bigcirc\text{-- }\bigcirc$	$H = -2J_1[(\mathbf{S}_1 \cdot \mathbf{S}_2) + (\mathbf{S}_2 \cdot \mathbf{S}_3)] + g\mu_B(S_1^z + S_2^z + S_3^z)B$ $E(S_T, S_a, m) = -J_1[S_T(S_T+1) - S_a(S_a+1) - \frac{35}{4}] + g\mu_B m B$ $\mathbf{S}_T = \mathbf{S}_1 + \mathbf{S}_2 + \mathbf{S}_3, \quad \mathbf{S}_a = \mathbf{S}_1 + \mathbf{S}_3$ $0 < S_a < 5, \quad |S_a - \frac{5}{2}| < S_T < S_a + \frac{5}{2} \quad |m| \leq S_T$	$B_n = 2(n + \frac{5}{2})|J_1|/g\mu_B$ $n = 1, \ldots, 5$
Closed triplet $\bigcirc\text{--}\bigcirc$	$H = -2J_1[(\mathbf{S}_1 \cdot \mathbf{S}_2) + (\mathbf{S}_2 \cdot \mathbf{S}_3) + (\mathbf{S}_3 \cdot \mathbf{S}_1)] + g\mu_B(S_1^z + S_2^z + S_3^z)B$ $E(S_T, m) = -J_1[S_T(S_T+1) - \frac{105}{4}] + g\mu_B m B$ $\mathbf{S}_T = \mathbf{S}_1 + \mathbf{S}_2 + \mathbf{S}_3, \quad \mathbf{S}_a = \mathbf{S}_1 + \mathbf{S}_3$ $0 < S_a < 5, \quad |S_a - \frac{5}{2}| < S_T < S_a + \frac{5}{2}, \quad |m| \leq S_T$	$B_n = (2n + 1)|J_1|/g\mu_B$ $n = 1, \ldots, 7$

quantum states for each cluster type i given in Table I. The total magnetization is

$$M = \sum_i M_i + M_\delta . \qquad (2)$$

The contribution M_δ of clusters with four spins or more is obtained self-consistently using the Weiss molecular-field model,

$$\langle S_z \rangle = -S\mathcal{B}_S \left[\frac{Sg\mu_B}{kT} \left[B - \frac{2J_1 v}{g\mu_B} \langle S_z \rangle \right] \right] , \qquad (3)$$

and

$$M_\delta = - \left[\frac{A}{W} x \right] P_\delta g\mu_B \langle S_z \rangle . \qquad (4)$$

Here, $P_\delta = 1 - P_s - P_p - (P_{ot} + P_{ct})$, $\mathcal{B}_S(y)$ is the Brillouin function, and v represents the mean number of NN's for a given spin in these large clusters and is the only fitting parameter in our calculation. The calculated field dependences of the magnetization for the various types of clusters are displayed in Fig. 1(a).

The Faraday-rotation measurements[11] of the magnetization[12] were carried out using the pulsed-field facility at the MIT Francis Bitter National Magnet Laboratory (FBNML). Magnetic fields up to 60 T were furnished by a Cu/Nb metal-matrix microcomposite magnet[13] with a ~ 7-ms half-period. A cw krypton-ion-pumped dye laser was used as a light source and was guided to the sample through optical fibers.[14] The Bridgman-grown sample (with $x = 0.095 \pm 0.004$) was sandwiched between a linear polarizer and a flat mirror and placed in contact with the liquid helium in a helium Dewar.[15] A small amount of heating (a few kelvin) was observed during the rapid field increase of the up-field sweep, so the data were taken from the down-field part of pulses during which the sample temperature was close to the bath temperature (~ 4

K). The dye laser was tuned to 1.55 eV (800 nm) to approach the resonant condition.

The experimental magnetic field dependence of the total magnetization M at ~ 4 K is displayed in Fig. 1(b), together with the theoretical calculation from Eq. (2). To deduce M from the Faraday angle θ, we calibrated the sample by separate dc-magnetization measurements to 20 T at 4.2 K using the high-field vibrating-sample magnetometer (VSM) facility of FBNML. In the calculation the experimental exchange energy $J_1/k_B = -6.1$ K is taken as an input constant.[16] We observe good overall agreement between experiment (solid points) and theory (solid curve), with the fitting parameter of Eq. (3), $v = 5.0$. As indicated by the arrows, two kinks are revealed in these high-field data. As the magnetic field increases, $M(B)$ increases linearly in the range from 15 to ~ 30 T with slope $\gamma_1 \equiv dM/dB$. It then switches to another region with larger slope γ_2. [In a previous measurement[12] up to 35 T, overall linear dependences of $M(B)$ versus B were observed for high manganese concentrations. However, for $x = 0.1$ there was a slight deviation from linearity starting at ~ 30 T.] As the field crosses ~ 50 T, the curve bends down into a linear slope, $\gamma_3 < \gamma_1$. These slope changes are directly related to the internal quantum structures of different clusters. To illustrate this point, we compare the data to the contributions from each component in Fig. 1(a). At $T = 4$ K, for each cluster type the discrete steps are broadened into a linear increasing ramp. For the manganese concentration and the field range of interest, since the large-cluster contribution M_δ is proportional to B and is the only component affected by parameter v, adjusting v only affects overall slope. Thus it is clear that the observed behavior of the magnetization originates from the pairs and open triplets. At approximately 30 T, open triplets announce their onset by an increase in slope (as indicated by the arrow). This gives rise to the upward turn in Fig. 1(b). The
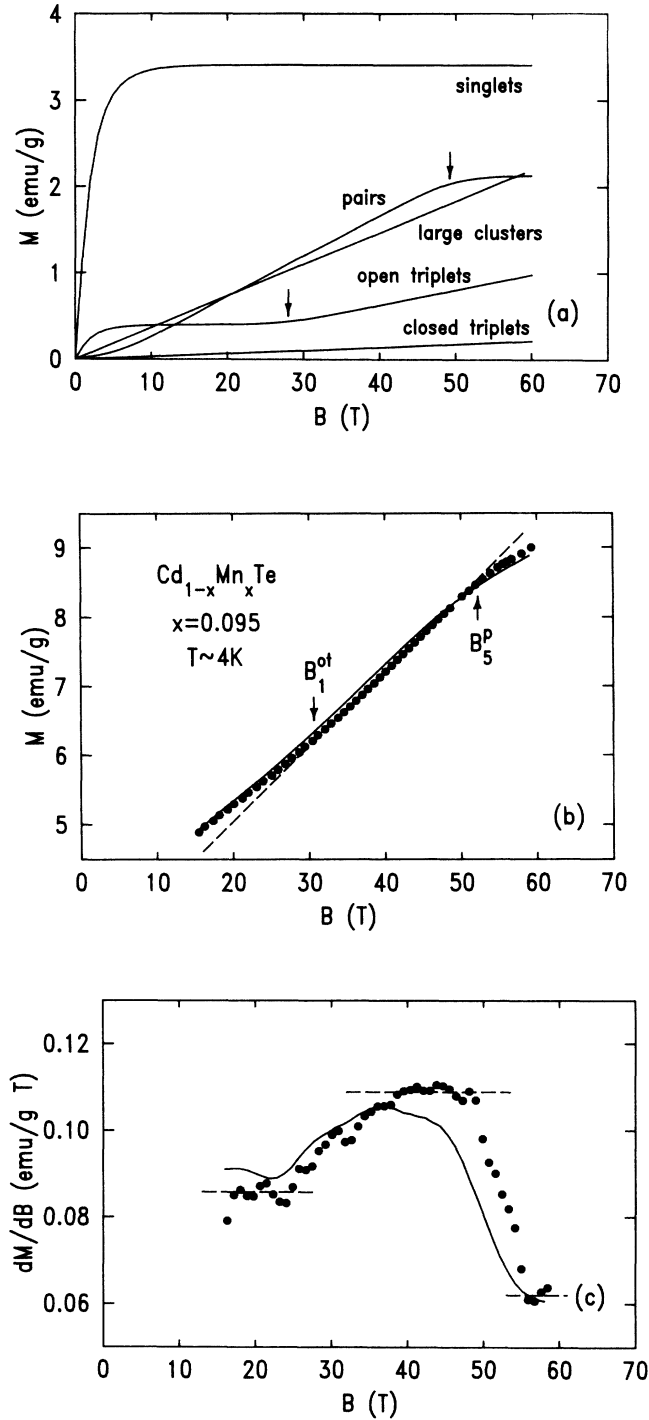
FIG. 1. Comparison of experimental and theoretical magnetization M as a function of applied magnetic field B in the range 15 to 60 T at $T \sim 4$ K for $Cd_{1-x}Mn_xTe$, $x = 0.095$. Experimental data are shown by solid points (one point per 90° Faraday rotation) and the theory is shown by the solid lines. The arrows near 30 T show the onset of triplet clusters and the arrows near 50 T show the saturation of pair clusters. (a) Numerical calculation for singlets, pairs, triplets, and large clusters in the nearest-neighbor cluster model. (b) Pulse-field magnetization measured by Faraday rotation. The dashed straight line is used as a reference for the slope changes. (c) First derivative of magnetization. The experimental data are smoothed.

downward turn at ~ 52 T is attributed to the pair's saturation.

Motivated by the qualitative interpretation of the experimental results discussed above, we now examine the quantitative details. Figure 1(c) is the derivative of magnetization dM/dB versus applied field B. (The small oscillating structure along the solid curve representing the theory is due to the pair steps, which is not our focus here.) The three plateaus shown by the dashed lines give γ_1, γ_2, and γ_3. Thus, according to the present model, the intrinsic probabilities for pairs and open triplets can easily be derived:

$$P_p = 2\alpha\gamma_p = 2\alpha(\gamma_2 - \gamma_3) \; ,$$
$$P_{ot} = 3\alpha\gamma_{ot} = 3\alpha(\gamma_2 - \gamma_1) \; , \tag{5}$$

where α is a constant for a given sample and has the form $\alpha = 2|J_1|W/[(g\mu_B)^2 Ax]$ in the NN model. The onset field for open triplets, B_1^{ot}, and the saturation field for pairs, B_5^p, are defined here by the point at which dM/dB equals the midpoints $(\gamma_1 + \gamma_2)/2$ and $(\gamma_2 + \gamma_3)/2$, respectively. The measured and calculated values of these quantities are compared in Table II. The reasonable agreement of the probabilities is consistent with the assumption that Mn ions are randomly distributed on the cation sublattice. However, the measured B_1^{ot} and B_5^p are larger than the predicted values in the NN model. This discrepancy is caused by the existence of a bias field,[4] i.e., the effective field experienced by a given cluster due to magnetic ions at distances beyond NN. In the present experiment with higher x and higher B than previous pair-step experiments, this bias field is more pronounced. Below, we examine this effect in more detail.

To measure the step fields B_n directly, dc-magnetization measurements using the high-field VSM up to 20 T were extended to 0.6 K. The obtained first and second[17] step fields B_1^p and B_2^p are also listed in Table
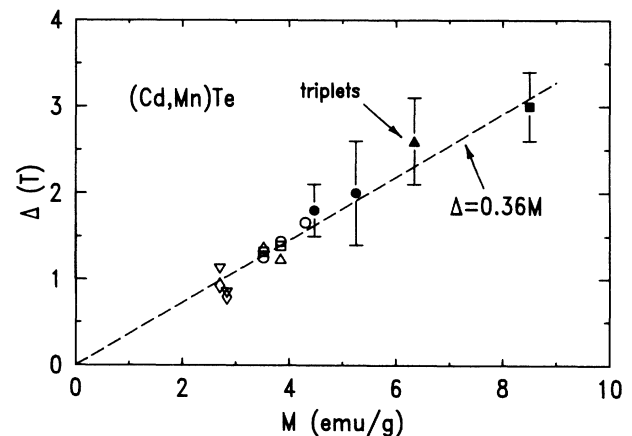

FIG. 2. Magnetization dependence of the bias field Δ for pairs and triplets for various x and T. For pairs: $x = 0.033$ at $T = 1.3$ K ($\Diamond$) and $T = 1.28$ K (∇) (Ref. 7); $x = 0.047$ at $T = 1.3$ K ($\triangle$) and $T = 0.47$ K ($\square$) (Ref. 3), and $T = 1.4$ K ($\circ$) (Ref. 8); $x = 0.095$ at $T = 0.6$ K ($\bullet$) and $T \sim 4$ K ($\blacksquare$) (this work). For triplets: $x = 0.095$ at $T \sim 4$ K ($\blacktriangle$) (this work). Typical error bars are shown here. The data include those obtained at different steps of the same sample.

TABLE II. Comparison of the measured and calculated probabilities (P) that an ion belongs to small clusters, and the transition fields B_n for the sample $Cd_{1-x}Mn_xTe$, $x = 0.095$. In the calculation, $J_1/k_B = -6.1$ K is taken as an input constant and further-neighbor interactions are neglected.

	P_p	P_{ot}	P_{ct}	B_1^{ot} (T)	B_5^q (T)	B_1^q (T)	B_5^q (T)
Meas.	0.19±0.02	0.14±0.02		30.6±0.5	52.2±0.4	10.9±0.3	20.2±0.6
Calc.	0.19	0.10	0.02	28.0	49.2	9.1	18.2

II. Comparing the bias field $\Delta_n \equiv B_n(\text{meas}) - B_n(\text{NN calc})$ at the first step of the pairs, $\Delta_1^p = 1.8$ T, to $\Delta_5^q = 3.0$ T at the saturation field of pairs, the ratio is $\Delta_5^q/\Delta_1^p \sim 1.7$. This is close to the ratio of magnetizations $M(B_5^q)/M(B_1^p) \sim 1.9$. Indeed, we expect the bias field to be proportional to the total magnetization. To further test this supposition, all available data on Δ versus M for $Cd_{1-x}Mn_xTe$ are collected and plotted in Fig. 2. These include the data obtained at different steps of the same sample. Despite the difference in manganese concentrations (which varies from $x = 0.033$ to $x = 0.095$), a *single* linear relation between Δ and the total magnetization M for pairs is observed,

$$\Delta = cM \ . \tag{6}$$

This general relation is useful for obtaining more accurate NN exchange constants for materials with sizable differences in magnetization between two adjacent steps. The empirical formula in Fig. 2 for $Cd_{1-x}Mn_xTe$ has the coefficient

$$c = 0.36 \pm 0.04 \text{ g T/emu} \ .$$

The positive sign of c indicates the overall negative exchange interaction for further neighbors. For different materials, c varies considerably due to the variation of the exchange interactions.

With the value of c, we can derive the NNN exchange constant within the mean-field model. In the mean-field theory the bias field for pairs is given by[4]

$$\Delta = -\tfrac{1}{2}(h_{1z} + h_{2z}) \ , \tag{7}$$

where

$$g\mu_B h_{pz} = -2\sum_q J(p,q)\langle S_{qz}\rangle \ ,$$

and $J(p,q)$ is the exchange constant between spins at sites p and q. The summation is over all sites q except nearest neighbors. Assuming that, on average, the two spins in a pair have equivalent paramagnetic environments, the bias field may be written as

$$\Delta = \sum_{r\geq 2} N_r J_r \frac{x\langle S_z\rangle}{g\mu_B}$$

$$= -\sum_{r\geq 2} N_r J_r \left[\frac{M}{(g\mu_B)^2(A/W)}\right] \ , \tag{8}$$

where N_r is the number of rth neighbors for *pairs* and J_r is the rth-neighbor exchange constant. Combining Eqs. (6) and (8), we obtain

$$c = -\left[\frac{W}{(g\mu_B)^2 A}\right] \sum_{r\geq 2} N_r J_r \ . \tag{9}$$

Note that c is independent of temperature T, and weakly dependent on x through W. To estimate J_2, the form $J_{(r>2)} = J_2(\sqrt{2}/r)^7$ (Ref. 18) is assumed. We find $J_2/k_B = -1.1\pm0.2$ K from the values -1.2 K when interactions up to third neighbors, and -1.1 K for interactions up to fourth neighbors are included. The error due to the uncertainty in c is also included. These values are comparable to the approximate value $J_2/k_B = -1.9\pm1.1$ K from Ref. 4. In Fig. 2 we also present the single data point for triplets of this work, which appears slightly above the empirical line for pairs.

In summary, we provide *quantitative evidence* of triplet ion clusters in DMS. Mn^{2+}-pair saturation is observed at ~ 52 T. Quantitative agreement between our experiment and calculations using the nearest-neighbor cluster model is obtained. The linear dependence of the bias field on the total magnetization derived here is consistent with the mean-field model. These results give important information on interactions beyond nearest neighbors.

---

*Also at Department of Physics, Massachusetts Institute of Technology, Cambridge, MA 02139.

[1]Y. Shapira, S. Foner, D. H. Ridgley, K. Dwight, and A. Wold, Phys. Rev. B **30**, 4021 (1984).

[2]R. L. Aggarwal, S. N. Jasperson, Y. Shapira, S. Foner, T. Sakakibara, T. Goto, N. Miura, K. Dwight, and A. Wold in *Proceedings of the 17th International Conference on Physics of Semiconductors*, edited by J. D. Chadi and W. A. Harrison

(Springer, New York, 1985), p. 1419.

[3]Y. Shapira and N. F. Oliveria, Jr., Phys. Rev. B **35**, 6888 (1987).

[4]B. E. Larson, K. C. Hass, and R. L. Aggarwal, Phys. Rev. B **33**, 1718 (1986).

[5]R. R. Galazka, W. Dobrowolski, J. P. Lascaray, M. Nawrocki, A. Bruno, J. M. Broto, and J. C. Ousset, J. Magn. Magn. Mater. **72**, 174 (1988), and references therein.

[6]N. Yamada, S. Takeyama, T. Sakakibara, T. Goto, and N. Miura, Phys. Rev. B **34**, 4121 (1986), and references therein.

[7]E. D. Isaacs, D. Heiman, P. Becla, Y. Shapira, R. Kershaw, K. Dwight, and A. Wold, Phys. Rev. B **38**, 8412 (1988).

[8]S. Foner, Y. Shapira, D. Heiman, P. Becla, R. Kershaw, K. Dwight, and A. Wold, Phys. Rev. B **39**, 11 793 (1989), and references therein.

[9]M. M. Kreitman, F. J. Milfort, R. P. Kenan, and J. G. Daunt, Phys. Rev. **144**, 367 (1966); S. Nagata, R. R. Galazka, D. P. Mullin, H. Akbarzadeh, G. D. Khattak, J. K. Furdyna, and P. H. Keeson, Phys. Rev. B **22**, 3331 (1980).

[10]R. E. Behringer, J. Chem. Phys. **29**, 537 (1958).

[11]J. A. Gai, R. R. Gałazka, and M. Nawrocki, Solid State Commun. **25**, 193 (1978); D. U. Bartholomew, J. K. Furdyna, and A. K. Ramdas, Phys. Rev. B **34**, 6943 (1986).

[12]D. Heiman, E. D. Isaacs, P. Becla, and S. Foner, Phys. Rev. B **35**, 3307 (1987).

[13]S. Foner, Appl. Phys. Lett. **49**, 982 (1986); Physica B+C **155B**, 18 (1989).

[14]D. Heiman, X. L. Zheng, S. Sprunt, B. B. Goldberg, and E. D. Isaacs, Proc. SPIE **1055**, 96 (1989).

[15]D. Heiman, Rev. Sci. Instrum. **56**, 684 (1985).

[16]The value of J_1 obtained at low ($x=0.033$) is used because the bias field arises primarily from singlets which are fully aligned and is thus nearly independent of the steps.

[17]We obtain the field corresponding to the second step, although the field was not high enough to fully resolve it, by assuming it has the same height and width as the first step.

[18]W. J. M. de Jonge, A. Twardowski, and C. J. M. Denissen, in *Diluted Magnetic Semiconductors,* Mater. Res. Soc. Symp. Proc. No. 89, edited by R. L. Aggarwal, J. K. Furdyna, and S. von Molnar (MRS, Pittsburgh, 1987), p. 153.